Molecular Structure of Three Mutations at the Maize *sugary1* Locus and Their Allele-Specific Phenotypic Effects[1]

Jason R. Dinges, Christophe Colleoni, Alan M. Myers, and Martha G. James*

Department of Biochemistry, Biophysics, and Molecular Biology, Iowa State University, Ames, Iowa 50011

Starch production in all plants examined is altered by mutations of isoamylase-type starch-debranching enzymes (DBE), although how these proteins affect glucan polymer assembly is not understood. Various allelic mutations in the maize (*Zea mays*) gene *sugary1* (*su1*), which codes for an isoamylase-type DBE, condition distinct kernel phenotypes. This study characterized the recessive mutations *su1-Ref*, *su1-R4582::Mu1*, and *su1-st*, regarding their molecular basis, chemical phenotypes, and effects on starch metabolizing enzymes. The *su1-Ref* allele results in two specific amino acid substitutions without affecting the Su1 mRNA level. The *su1-R4582::Mu1* mutation is a null allele that abolishes transcript accumulation. The *su1-st* mutation results from insertion of a novel transposon-like sequence, designated *Toad*, which causes alternative pre-mRNA splicing. Three *su1-st* mutant transcripts are produced, one that is nonfunctional and two that code for modified SU1 polypeptides. The *su1-st* mutation is dominant to the null allele *su1-R4582::Mu1*, but recessive to *su1-Ref*, suggestive of complex effects involving quaternary structure of the SU1 enzyme. All three *su1-* alleles severely reduce or eliminate isoamylase-type DBE activity, although *su1-st* kernels accumulate less phytoglycogen and Suc than *su1-Ref* or *su1-R4582::Mu1* mutants. The chain length distribution of residual amylopectin is significantly altered by *su1-Ref* and *su1-R4582::Mu1*, whereas *su1-st* has modest effects. These results, together with *su1* allele-specific effects on other starch-metabolizing enzymes detected in zymograms, suggest that total DBE catalytic activity is the not the sole determinant of *Su1* function and that specific interactions between SU1 and other components of the starch biosynthetic system are required.

Much of the metabolic activity in plants is directed toward production of starch from reduced carbon formed during photosynthesis. Starch that accumulates in leaves during the light phase of a diurnal cycle is degraded in the dark phase. Suc is transported from this source tissue to non-photosynthetic storage tissues, where it supplies Glc units for the synthesis of starch that serves as the carbon reserve for the subsequent generation. Starch biosynthesis is highly conserved throughout the plant kingdom, presumably owing to this central role in plant physiology and reproduction. Nevertheless, there is little understanding of the molecular mechanisms that determine how the precise structure of starch is achieved in either leaves or storage tissues.

Starch comprises two homopolymers of Glc, amylopectin, and amylose, and it is the ordered architectural structure of amylopectin, the most abundant component, that confers crystallinity to the starch granule (Imberty et al., 1991; Gallant et al., 1997). Amylopectin synthesis involves the combined actions of multiple isoforms of starch synthases (SS), which elongate linear chains via the introduction of α-(1→4) glycosidic bonds, and starch branching enzymes (BE), which catalyze the formation of α-(1→6) branch linkages (for reviews, see Smith, 1999; Kossman and Lloyd, 2000; Myers et al., 2000). The nonrandom placement of branch linkages and determination of chain length results in a complex, hierarchical structure that renders the molecule both crystalline and insoluble.

A broad body of genetic evidence in several plant species indicates that α-(1→6) glucan hydrolases, i.e. starch debranching enzymes (DBE), are necessary for the normal formation of crystalline starch granules. Two types of DBEs have been identified in plants, distinguished by their substrate specificities (Lee and Whelan, 1971; Doehlert and Knutson, 1991). Isoamylase-type DBEs cleave α(1→6) branch linkages in amylopectin and glycogen, but do not hydrolyze the chemically identical bonds in pullulan, an α(1→6)-linked maltotriose polymer. In contrast, pullulanase-type DBEs, also referred to as R-enzymes or limit-dextrinases (Manners, 1997), hydrolyze α(1→6) linkages of pullulan and to a lesser degree amylopectin, but have little or no activity toward glycogen. Sequence comparisons among plant and bacterial α(1→6) glucan hydrolases indicate that the pullulanase-type and isoamylase-type DBEs have been conserved separately in evolution (Beatty et al., 1999).

[1] This work was supported by the U.S. Department of Agriculture (grant no. 99–35304–8642 to M.G.J. and A.M.M.), by a U.S. Department of Agriculture National Needs Fellowship in Plant Biotechnology (grant no. 98–38420–5838 to J.R.D.), and by the National Science Foundation (grant no. DIR–9113593 to the Iowa State University Signal Transduction Training Group). This is a journal paper (no. J–19209) of the Iowa Agriculture and Home Economics Experiment Station (Ames; project no. 3593).

* Corresponding author; e-mail mgjames@iastate.edu; fax 515–294–0453.

The first genetic evidence for DBE involvement in starch biosynthesis came from mutations of the maize (*Zea mays*) *sugary1* (*su1*) gene, described a century ago in the scientific literature (Correns, 1901). These mutations result in the accumulation of soluble sugars and a water-soluble polysaccharide (WSP) termed phytoglycogen in the kernel (Morris and Morris, 1939). In *su1* kernels, the reduction in amylopectin content approximately matches the abundance of phytoglycogen, suggesting a diversion from biosynthesis of the normal insoluble branched glucan to the water-soluble form. Similar to glycogen, phytoglycogen has approximately twice the frequency of branch linkages as amylopectin, a shorter average chain length, and a more uniform chain length distribution (Yun and Matheson, 1993). More recently, the accumulation of phytoglycogen also has been reported in mutants of rice, Arabidopsis, and *Chlamydomonas* (Mouille et al., 1996; Nakamura et al., 1996; Zeeman et al., 1998; Kubo et al., 1999). In each species, phytoglycogen accumulation correlates with a lack of DBE activity of the isoamylase type (Mouille et al., 1996; Rahman et al., 1998; Zeeman et al., 1998; Beatty et al., 1999; Kubo et al., 1999). In maize and Arabidopsis the mutation responsible for this specific phenotype has been shown directly to reside in a gene that codes for an isoamylase-type DBE (James et al., 1995; Zeeman et al., 1998), and indirect evidence indicates this is likely to be the case in *Chlamydomonas* and rice.

The first described *su1* mutation (Correns, 1901) is now termed *su1-Ref*. As the allele name indicates, this mutation has served as the reference standard for most analyses of the phenotypic effects. Kernels homozygous for *su1-Ref* have a glassy, translucent, and shrunken appearance at maturity resulting from their altered carbohydrate composition. The total amount of phytoglycogen reported to be present in *su1-Ref* kernels has ranged from 25% to 35% of the total glucan (Creech, 1968; Shannon and Garwood, 1984). Several early reports indicated that *su1-Ref* kernels contained an altered BE activity, prompting speculation that phytoglycogen accumulation results from an alteration in the formation of branch linkages (Lavintman, 1966; Manners et al., 1968; Hodges et al., 1969; Tomalsky and Krisman, 1987). Previous analysis of *su1-Ref* mutant kernels also revealed the deficiency of a DBE, although that activity was of the pullulanase-type (Pan and Nelson, 1984). More recently, cloning of the *Su1* gene revealed that it codes for a DBE of the isoamylase-type (James et al., 1995), and that *su1-Ref* kernels are deficient in both isoamylase- and pullulanase-type DBE isoforms (Beatty et al., 1999). This dual effect on both DBEs is also observed in endosperm tissue of rice *su1* mutants (Nakamura et al., 1996). However, pullulanase-type DBE apparently is unaffected in Arabidopsis leaves or the unicellular algae *Chlamydomonas* when mutations affecting an isoamylase-type DBE are present (Zeeman et al., 1998; Dauvillee et al., 2000).

The complexity of the starch biosynthetic system, including the involvement of multiple isozymes of SS, BE, and DBE, so far has precluded biochemical reconstitution of an architecturally accurate synthetic system. Pleiotropic effects in most phytoglycogen-accumulating mutants also have complicated the analysis of the role of isoamylase-type DBEs in the starch biosynthetic process. In this study, we have begun to exploit the great deal of allelic diversity that is available for the maize *su1* locus, toward the aim of establishing correlations between mutational effects on the SU1 polypeptide, specific enzymatic alterations, and defined changes in the chemical structures of glucan polymers. Three *su1* alleles in near-isogenic lines were compared with the nonmutant allele *Su1*. Two of the mutant alleles, *su1-Ref* and the transposon-induced allele *su1-R4582::Mu1* (James et al., 1995), condition severe glassy, shrunken, and translucent kernel phenotypes. The third, *su1-starchy* (*su1-st*), results in a relatively mild phenotype in which translucency is typically limited to the kernel crown (Dahlstrom and Lonnquist, 1964). This research examined the dominance relationships among these *su1* alleles, the quantity of phytoglycogen and sugars that accumulate in the kernels, the chain length distributions of the polymers present, and the effects of each allele on the activities of DBEs and other starch metabolizing enzymes. The molecular nature of each mutation also was determined. In the course of this analysis, a novel transposon-like sequence, termed *Toad*, was identified at the *su1-st* locus. This element was shown to affect the pre-mRNA splicing of the exon in which it resides. The three *su1-* mutations had diverse effects on the compositions and structures of kernel glucans, as well as on the activities of other starch metabolizing enzymes. However, direct correlation was not established between the apparent level of isoamylase-type DBE activity and the observed chemical phenotype. Together, the findings suggest that the effects of each mutation varied according to the primary structure of the SU1 polypeptide, and may relate to the assembly-state of the SU1 holoenzyme.

RESULTS

Kernel Morphologies and Dominant/Recessive Relationships of the *su1-* Mutations

Self-pollinated ears from *Su1/su1-Ref* or *Su1/su1-st* heterozygous plants contain progeny kernels segregating at the ratio of 1:3 for the mutant and nonmutant phenotypes. The typical glassy, shrunken, and translucent phenotype of *su1-Ref* homozygous kernels is evident (Fig. 1A), and this is very similar to the kernel phenotype conditioned by *su1-R4582::Mu1* (James et al., 1995). The *su1-st* kernel phenotype is relatively slight (Fig. 1B) compared with that conditioned by *su1-Ref*. These mutant kernels are plump and starchy with translucency and wrinkling only on

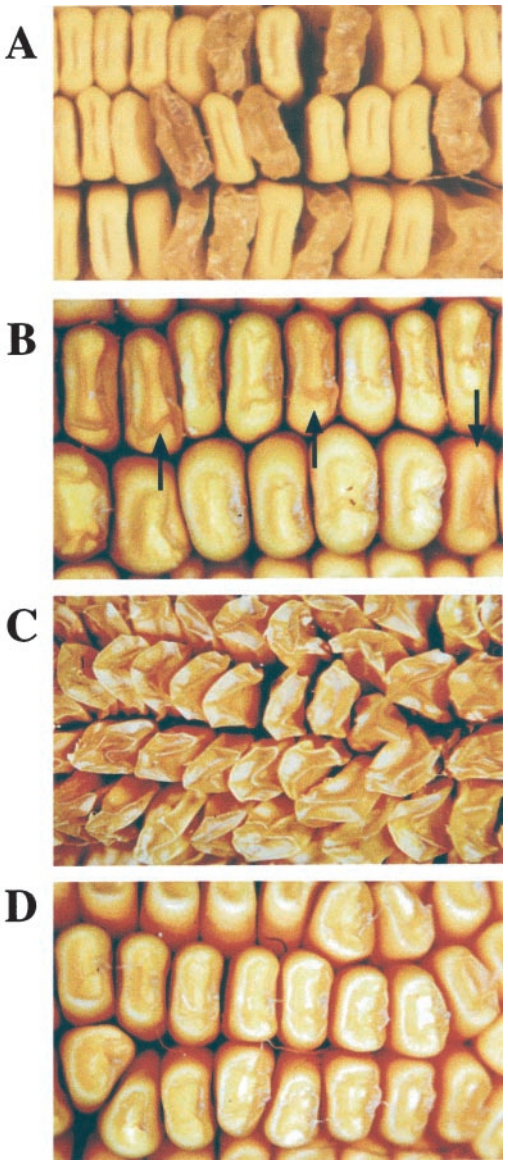

Figure 1. Kernel phenotypes of *su1*-mutants. A, The *su1-Ref* mutant phenotype. The ear shown was obtained by self-pollination of an *su1-Ref/Su1* heterozygote. B, The *su1-st* mutant phenotype. The ear shown was obtained by self-pollination of an *su1-st/Su1* heterozygote. Mutant kernels (examples indicated by the arrows) and wild-type kernels segregated at a frequency of approximately 1:3, respectively. C, Phenotype of *su1-Ref/su1-st* kernels. The ear shown is the result of a cross of an *su1-st/su1-st* plant as the male parent to an *su1-Ref/su1-Ref* plant as the female parent. D, Phenotype of *su1-R4582::Mu1/su1-st* kernels. The ear shown is the result of a cross of an *su1-R4582::Mu1/su1-R4582::Mu1* plant as the male parent to an *su1-st/su1-st* plant as the female parent.

the kernel crown. Also, the *su1-st* mutation varies considerably in expressivity with some kernels appearing near normal. Despite these distinct kernel phenotypes, *su1-st* is clearly identified as a mutation of the *su1* locus because it fails to complement *su1-Ref* and by definitive molecular characterization (see following section).

Previous genetic analyses of the dominant/recessive relationship between *su1-st* and wild-type (*Su1*) or *su1-Ref* alleles showed that the *su1-st* allele is recessive to both, although reciprocal crosses between *su1-Ref* and *su1-st* plants indicated subtle dosage effects of the *su1-st* allele (Dahlstrom and Lonnquist, 1964). This finding also was confirmed in this study, where progeny ears from reciprocal *su1-Ref* by *su1-st* crosses produced kernels that were uniformly shrunken, glassy, and translucent in appearance (Fig. 1C). Crosses also were made between *su1-st* plants and plants homozygous for *su1-R4582::Mu1*. The *su1-R4582::Mu1* allele is predicted to be a null allele, based on the presence of a *Mu1* transposable element in the first exon of the gene downstream of the translational start site (James et al., 1995). Progeny ears from the *su1-st* by *su1-R4582::Mu1* cross were uniformly like *su1-st* homozygotes in appearance, indicating that the *su1-st* allele is dominant to *su1-R4582::Mu1* (Fig. 1D). Given that *su1-Ref* and *su1-R4582::Mu1* condition nearly identical kernel phenotypes, the different dominance relationships of these two alleles with *su1-st* most likely reflect the presence or absence of a SU1 polypeptide.

Steady-State Levels of Su1 mRNA in the Various *su1*- Mutants

Gene expression of *su1-Ref*, *su1-st*, and *su1-R4582::Mu1* relative to the nonmutant allele *Su1* was characterized in kernels at a mid-developmental stage by RNA gel-blot analysis. Total RNA was isolated from kernels harvested 20 DAP and hybridized with an antisense RNA probe from the 3′ end of the Su1 cDNA. Kernels homozygous for *su1-Ref* produce transcripts of normal size that accumulate to wild-type levels (Fig. 2). In contrast, kernels homozygous for *su1-R4582::Mu1* accumulated no detectable Su1 transcript. This supports the prediction that *su1-R4582::Mu1* is a null allele. Homozygous *su1-st* kernels at this stage accumulated a relatively slight amount of apparently normal-sized transcript. Thus, the partial function of the *su1* locus that is evident from the intermediate phenotype conditioned by *su1-st* (Fig. 1; Table I) is provided by a relatively small number of transcripts.

The Molecular Nature of *su1-Ref*

Although the *su1-Ref* mutation has long been used for the production of traditional sweet corn varieties, the molecular basis for this mutation was not known. To characterize this allele, segments of *su1-Ref* kernel mRNA and genomic DNA were amplified by PCR, and their sequences were determined. All materials analyzed were obtained initially from the W64A genetic background. Sequence comparisons of *su1-Ref* to *Su1* revealed three nucleotide changes that would result in amino acid substitutions, a C to G transversion at nucleotide (nt) 576, an A to G transition at nt 1,100, and a T to C transition at nt 1,819 (nucleotide

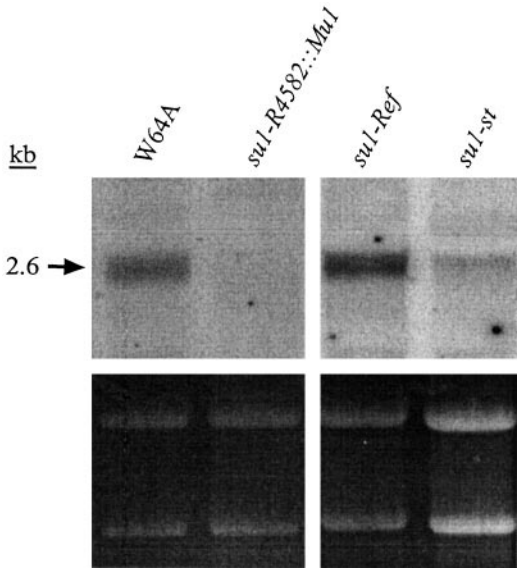

Figure 2. RNA gel-blot analysis. Total RNA was extracted from endosperm of kernels harvested at 20 DAP, fractionated on a 1% (w/v) agarose-formaldehyde gel, and hybridized with Su1 cDNA antisense RNA. RNA concentration variations can be visualized by the ethidium bromide-stained rRNA, shown in the lower panel. The lanes shown were run simultaneously in the same gel.

and amino acid numbers refer to GenBank accession no. U18908). Translation would result in three amino acid changes relative to the wild-type polypeptide SU1, Phe to Leu at residue 163, Glu to Val at residue 338, and Trp to Arg at residue 578. This mutant polypeptide is designated $SU1^{Ref}$. Similar analysis of commercial *su1-Ref* sweet corn varieties in the NK199 and Golden Cross Bantam backgrounds showed that only two of these nucleotide changes were present, specifically those resulting in the F163L and W578R substitutions. These two mutations, therefore, most likely were present in the progenitor *su1-Ref* allele that has been used in existing commercial sweet corn lines and introgressed into the inbred line W64A. The third mutation, E338V, most likely arose more recently and thus is not required for the phytoglycogen-accumulating phenotype conditioned by *su1-Ref*.

Sequence comparisons among α-(1→6) glucan hydrolases revealed numerous conserved sequence blocks, some of which are common to all members the α-amylase family (Jesperson et al., 1993) and some of which are specific to either the isoamylse-type or pullulanase-type DBE isoforms (Beatty et al., 1999). Two of the three substitutions in *su1-Ref* occur within conserved domains, specifically E338V in α-amylase region I, and W578R in the isomylase-specific domain IS-XII. The third mutation, F163L, lies just downstream of domain IS-VII but is not located in a conserved region of the enzyme. The only highly conserved residue affected in *su1-Ref* is W578, which is present in all isoamylases examined to date from plants and bacteria except that from *Escherichia coli* (Beatty et al., 1999). W578R, therefore, is likely to cause the defect in the SU1 isoamylase-type DBE in *su1-Ref* mutants.

Structure of the mRNA Transcripts from *su1-st*

The molecular nature of the *su1-st* mutation also was characterized, again beginning with reverse transcriptase (RT)-PCR amplification of mRNA from homozygous mutant kernels. Primers 797 and JD02 from the Su1 cDNA sequence, which correspond to regions within exon 3 and exon 11 of the genomic sequence, respectively, were predicted to amplify a fragment of 800 bp (Beatty et al., 1997) (Fig. 3A). For *Su1* and *su1-Ref*, a fragment of the predicted size was amplified (Fig. 3B, lane 1; and data not shown). The major RT-PCR product from *su1-st* kernels, however, was approximately 100 bp smaller than that obtained from wild-type kernels, although a minor product near the expected size also was seen (Fig. 3B, lane 2). Sequence analysis of the approximately 700-bp major product revealed that in this mutant mRNA, the splice donor site of exon 9 has been joined precisely to the acceptor site of exon 11, and that exon 10 is completely lacking. Loss of this 127-nucleotide exon would result in a shift in the open reading frame within exon 11 and the introduction of a premature translational stop codon. Therefore, this transcript, designated as transcript type I, is predicted to result in the translation of a truncated, nonfunctional polypeptide.

The preceding observation was difficult to reconcile with the fact that *su1-st* mutants display a kernel morphology and chemical phenotype quite distinct from those of the confirmed null mutation *su1-R4582::Mu1* (Fig. 1; Table I). To search for minor transcripts in which exon 9 was correctly spliced to exon 10, a RT-PCR primer that bridges this splice donor site and acceptor site was synthesized. Kernel RNA was amplified by RT-PCR using this primer, JD18, and the downstream primer JD03 from within exon 16 (Fig. 3A). This resulted in two distinct *su1-st* mutant cDNA products, one slightly smaller than that obtained when *Su1* kernel RNA was amplified with this primer pair, and the other slightly larger (Fig. 3B, lanes 3 and 4). These two transcripts are designated type II and type III, respectively. The observation of multiple *su1-st* transcripts, none of which is the size of the wild-type transcript, suggests that alternative splicing occurs in pre-mRNA transcripts from the *su1-st* locus.

To further investigate the apparent deletion of exon 10 in transcript I, genomic DNA from a homozygous *su1-st* plant was amplified with oligonucleotide primers JD19 and JD20, derived from intron 9 and intron 10, respectively. This primer pair is designed to amplify a sequence of 370 bp from wild-type genomic DNA that includes all 127 bp of exon 10 flanked by portions of the adjacent introns. The predicted amplification product was obtained from genomic DNA from a *Su1* plant, but a product of slightly greater than 1 kb was obtained from *su1-st*

Table I. *Carbohydrate analysis of nonmutant maize W64A kernels and sugary1 mutant kernels*

	Year	DAP	Total Carbohydrate										Total mg/g	% Glucan Polymer	
			Glc		Fru		Suc		WSP[a]		Starch[a]			WSP	Starch
			mg/g[b]	%	mg/g[b]	%	mg/g[b]	%	mg/g[b]	%	mg/g[b]	%			
W64A	2000	20	3.7	0.5	3.2	0.45	43	5.6	5.6	0.7	718	92.7	774	0.8	99.2
W64A	1999	30	2.4	0.3	2	0.2	31	3.6	15	1.8	820	94	870	2	98
sul-ref	2000	20	9.3	1.5	5.5	0.9	168	27.8	336	55.6	85	14.1	604	80	20
sul-ref	1999	30	20	3.8	4.4	0.8	109	20.5	274	52	121	22.8	528	70	30
sul-4582	1998	25	15	2	5.5	0.8	110	16	465	66.5	103	15	699	80	20
sul-st	2000	20	9.1	1.2	7.6	1	104	13.6	198	26	444	58	763	31	69
sul-st	1998	20	12	1.9	9.3	1.5	123	19.7	242	38.7	240	38.1	626	50	50
sul-st	1997	30	3.6	0.5	2.2	0.3	30	4	52	6.8	683	88.5	771	7	93

[a] The amount of WSP and starch were determined as glucose equivalents by measuring the amount of glucose produced following complete digestion with amyloglucosidase. [b] The results are expressed as milligram of carbohydrate by gram of dry wt.

genomic DNA (Fig. 3C). Characterization of this mutant fragment revealed the insertion of a 638-bp sequence within exon 10, as well as duplication of 10 nt of the *Su1* sequence flanking each end of the insertion (ATTACGACAG; Fig. 4). This 638-bp sequence is referred to as the "*Toad* " genetic element.

Characterization of the *su1-st* genomic sequence enabled definition of the pre-mRNA splicing events that gave rise to the type-II and type-III transcripts. Nucleotide sequence of the shorter cDNA amplified by the JD18/JD03 primer pair (Fig. 3B), corresponding to the type-II transcript, revealed deletion of 18 nt within exon 10 (Fig. 4). This deletion extends from nucleotide 5,248 in the *su1* genomic sequence through nucleotide 5,265 (GenBank accession no. AF030882). The latter nucleotide corresponds to the last residue of the direct repeat adjacent to both ends of the *Toad* element. This deletion maintains the open reading frame of the mRNA, resulting in a mutant polypeptide designated $SU1^{st\text{-}II}$, that has a deletion of six amino acids (residues 440–445; GDMITT). The larger cDNA product, corresponding to the type-III transcript, contains an insertion of 30 nt relative to the nonmutant sequence. This insertion corresponds exactly to the first 30 nt of the inserted *Toad* element. In this instance the reading frame is again maintained with the insertion of 10 amino acids of the sequence EIWNHAIMLR between residues 446 and 447 of the nonmutant protein, resulting in $SU1^{st\text{-}III}$. In the type-II transcript the entire *Toad* element contained in the genomic sequence is missing from the mRNA, and in the type-III transcript all but 30 nt of *Toad* have been removed. Thus it appears that the insertion or deletion mutations in the type-II and -III transcripts are generated through aberrant pre-mRNA splicing events induced by presence of the *Toad* element.

A Novel Transposon-Like Sequence within the *su1-st* Locus

The 638-bp insertion sequence found within exon 10 at the *su1-st* locus was subjected to a BLAST search

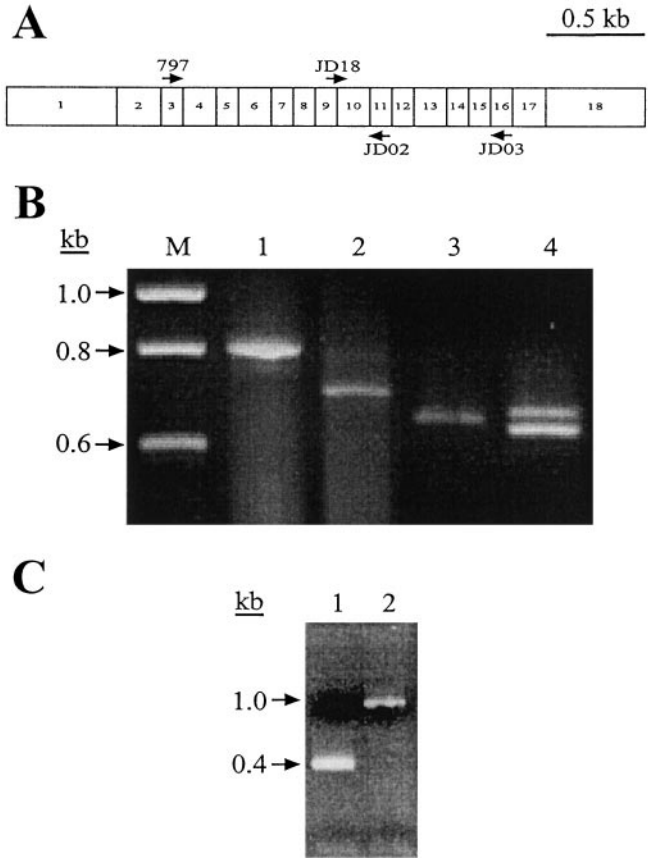

Figure 3. PCR and RT-PCR analyses. A, Relative positions of oligonucleotide primers within the Su1 cDNA. Exons comprising the Su1 cDNA are represented by numbered boxes. Primers used for the detection of alternatively spliced transcripts are indicated by arrows above and below the boxes (depicting sense and antisense sequences, respectively). B, RT-PCR amplifications. DNA was reverse-transcribed from purified mRNA isolated from 20 DAP whole kernels homozygous for *Su1* (lanes 1 and 3) and *su1-st* (lanes 2 and 4). Primer pair 797/JD02 was used for the amplifications in lanes 1 and 2, and primer pair JD03/JD18 was used for the amplifications in lanes 3 and 4. C, PCR amplification of genomic DNA from seedling tissue homozygous for *Su1* (lane 1) and *su1-st* (lane 2) with primer pair JD19/JD20 to amplify the region of the gene containing the *Toad* element.

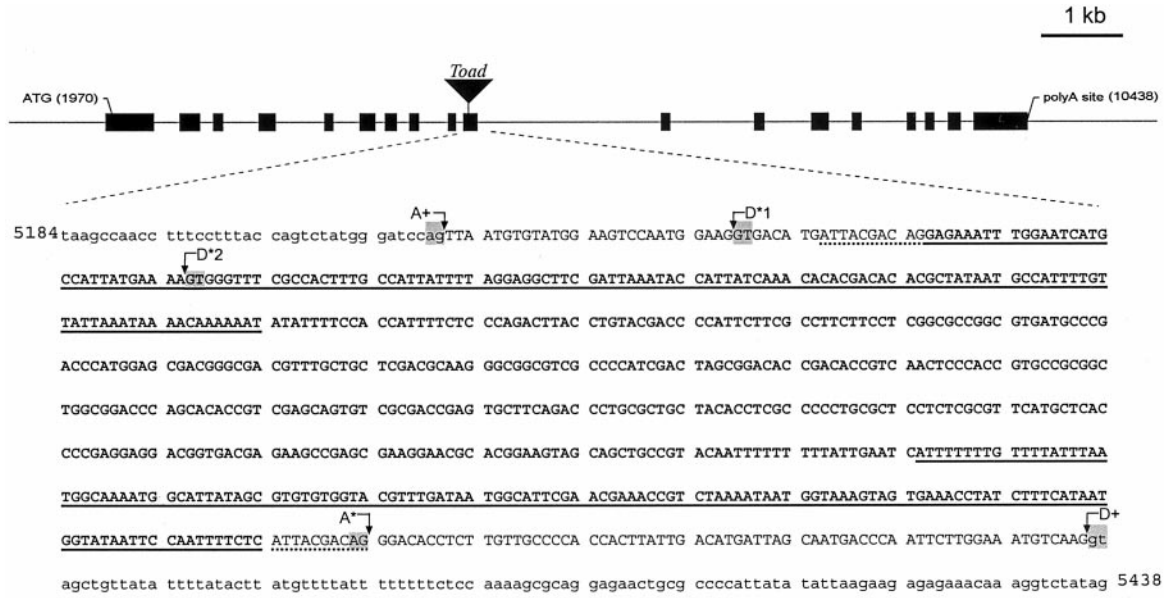

Figure 4. Nucleotide sequence analysis of the *su1-st* locus. The *su1-st* locus contains an insertion of the 638-bp *Toad* sequence (shown in bold) in exon 10. Intron sequence flanking exon 10 is designated by lowercase letters, and exon 10 sequence is designated by uppercase letters. Nucleotides underlined with a dotted line indicate the 10-bp target site duplication of the host sequence. Regions underlined with a solid line indicate 138-bp TIRs within the *Toad* element. The wild-type acceptor site for the end of intron 9 is designated A+. The intron formed for the creation of the type-II transcript is made by joining cryptic acceptor sites D*1 to A*. This results in a deletion of 18 nt of Su1 sequence from the mature transcript and complete removal of the *Toad* sequence. The intron formed for the type-III transcript is produced by the use of D*2 as the donor site and A* as the acceptor site, removing most of the *Toad* sequence as an intron, but leaving an insertion of 30 bp in the mature mRNA. The wild-type donor site for the start of intron 10 is indicated as D+. The highly conserved GT and AG dinucleotides found at the termini of most plant introns are highlighted at the indicated splice donor/acceptor sites. The nucleotides indicated correspond to the wild-type *Su1* genomic sequence (GenBank accession no. AF030882).

of the public databases. This search failed to identify similar sequences within any genome, indicating that the 638-bp sequence is novel. Alignment of the nucleotide sequence of the element with its reverse complement identified terminal inverted repeat (TIR) regions of 138 bp, which are 86% identical. Class-II transposable elements in flowering plants, which include all non-retrotransposons, are characterized by the presence of TIRs that range from a few to more than 200 nucleotides (Finnegan, 1989). Also, insertion of a class-II transposable element typically results in the duplication of small region of host DNA at the insertion site, such that direct host repeat sequences flank the element (Federoff, 1989). Together, these transposon-like features of *Toad* are strong indicators that the 638-bp sequence is a transposable element (the sequence of *Toad* is available as GenBank accession no. AF317693). Open reading frames of 67, 70, and 94 codons are present within *Toad*, although none of the predicted polypeptides are significantly similar to sequences in the public database.

To investigate the approximate number of copies of the *Toad* elements, or homologous elements, within the maize genome, DNA from six inbred lines was subjected to high stringency gel-blot analysis with the *Toad* sequence as a hybridization probe. This analysis indicated that *Toad* is a low-copy element with no more than two to four copies in any of the genomes tested (data not shown). In DNA from a *su1-st* plant, two *Toad* sequences were observed, one corresponding to the element at the *su1-st* locus and the other corresponding to the single *Toad* sequence in the W64A genome. A detailed analysis of the *Toad* sequence revealed short blocks of similarity with other maize transposons, such as have been observed for many plant transposable elements (Nevers et al., 1986).

Glucan Structure Phenotypes

The phenotype conditioned by each *su1-* mutation with regard to the chemical properties and structures of the glucans present in developing kernels was determined. Aqueous kernel extracts were prepared from samples harvested at mid-developmental time points from several growing seasons, and separated by centrifugation into soluble and granular phases. The quantities of Suc, D-Glc, D-Fru, oligosaccharide, and glucan polymer in each phase were determined by specific analytical methods (Table I). The carbohydrate profile conditioned by either *su1-R4582::Mu1* or *su1-Ref* is significantly altered relative to nonmutant kernels, whereas *su1-st* conditions an intermediate

phenotype. The intermediate effects of the *su1-st* allele varied, however, among the samples, suggesting environmental factors may impact *su1-st* phenotypic expression.

Selected data from Table I highlight *su1* allele-specific effects on carbohydrate composition. For example, approximately 4% of the total carbohydrate is in the form of Suc in both *Su1* and *su1-st* kernels harvested 30 d after pollination (DAP) from the 1997 nursery, but higher Suc proportions are found in 20-DAP *su1-st* kernels from the 1998 and 2000 nurseries, approximately 14% and approximately 20%, respectively. Suc comprises 16% of the total carbohydrate in *su1-R4582::Mu1* and approximately 20% to 28% of the total carbohydrate in *su1-Ref* kernels. The great majority of carbohydrate in nonmutant kernels at 20 or 30 DAP, approximately 94%, is in the form of starch. Granular starch is reduced to various levels in *su1-st* kernels, comprising approximately 88% of the 30 DAP sample from 1997, approximately 38% of the 20-DAP sample from 1998, and 58% of the 20-DAP sample from 2000. In contrast, only approximately 14% to 23% of the total carbohydrate in *su1-Ref* kernels and *su1-R4582::Mu1* kernels is found in starch granules at comparable developmental stages. The relative severity of the phenotypes also is evident in the accumulation of WSP (i.e. phytoglycogen). This more highly-branched glucan accounts for approximately 52% to 66% of the total carbohydrate in the more phenotypically severe *su1-R4582::Mu1* or *su1-Ref* kernels, whereas in *su1-st* kernels WSP comprised approximately 7% of the total in the 30 DAP sample and from 26 to approximately 39% in the 20 DAP samples.

The structure of the amylopectin purified from granules of each mutant was analyzed by high performance anion exchange chromatography with pulsed amperometric detection (HPAEC-PAD) to determine if the *su1-* mutations resulted in altered chain length distributions. Analysis of starch from 30-DAP kernels revealed that the amylopectin component in *su1-R4582::Mu1* and *su1-Ref* kernels is structurally different from wild-type amylopectin (Fig. 5A). The amylopectin-like glucans in *su1-R4582::Mu1* and *su1-Ref* kernels are similar to each other, having more short chains, approximately 3 to 12 glucosyl units in length, and fewer intermediate-length chains, approximately 12 to 30 glucosyl units in length, relative to wild type. The *su1-st* chain length profile for amylopectin is intermediate between wild type and that of *su1-R4582::Mu1* and *su1-Ref* with slightly more short chains and slightly fewer intermediate chains relative to wild type. Thus, the *su1-st* amylopectin-like glucan is structurally distinct from any of the others. A similar analysis of the WSP from *su1-Ref* and *su1-st* kernels also shows that these two soluble glucans have structural differences, as evidenced by a reduction in very short chains, less than six glucosyl units in length, in the *su1-st* WSP (Fig. 5B).

Enzyme Profile Phenotypes

To examine the pleiotropic effects of *su1* mutations on starch metabolizing enzyme activities, proteins from developing wild-type kernels and kernels homozygous for *su1-Ref*, *su1-R4582::Mu1*, and *su1-st* were separated by native PAGE and transferred to acrylamide gels containing solubilized starch. After incubation of the activity gels (i.e. zymograms) and staining with I_2/KI, enzymes that modify starch structure are detected by alterations in the dark blue background color. Thus, DBE activities are visualized as light blue-staining bands, BE activities as red- or orange-staining bands, and amylolytic activities as regions where staining is reduced to white or very light color. The *su1-R4582::Mu1* and *Su1* extracts were compared initially on 5-cm gels (Fig. 6A), which showed that a series of light blue bands was completely missing in the mutant extract. These bands did not appear when red-pullulan, a pullulanase-type DBE-specific substrate, was included in the activity gels (data not shown). Considering that *su1-R4582::Mu1* is a null mutation of a gene coding for an isoamylase-type DBE (see below), these data strongly suggest that the light blue bands represent the isoamylase activity coded for by *su1*.

All three mutants also were analyzed on 15-cm activity gels, which reveal a larger number of starch metabolizing enzymes (Fig. 6B). In the nonmutant extract, the isoamylase activity was observed as a series of diffuse, light-blue bands at the top of the gel. This broad staining area labeled as arrow A is not detected in any of the three *su1-* mutants, and the light blue band labeled as arrow B also is missing in the mutants. Notably, the pattern in this region of the gel is the same in all three *su1-* mutants. Another light blue band was evident in the 15-cm gels, noted by arrow E. Duplicate gels including red-pullulan as the substrate showed an activity band of the same electrophorectic mobility, demonstrating that this signal indicates the pullulanase-type DBE (data not shown). This pullulanase-type enzyme activity was reduced in all three mutants relative to wild type, consistent with previous characterizations of DBEs in *su1-Ref* (Pan and Nelson, 1984; Beatty et al., 1999) and *su1-* mutants of rice (Kubo et al., 1999).

The *su1-* mutations also result in a wide variety of allele-specific changes in other starch modifying activities, as exhibited by altered staining intensity or protein mobility. An apparent BE activity (Fig. 3B, arrow C), as indicated by the red color of the band, is increased in staining intensity in *su1-R4582::Mu1* and *su1-st* extracts compared with wild type, although this activity is not affected by *su1-Ref*. Also, a new apparent amylolytic activity, as suggested by the white color of the band, appears specifically in the *su1-R4582::Mu1* and *su1-st* mutants (arrow F). An unknown starch modifying activity (arrow D) is not detected specifically in *su1-st* extracts. Furthermore, a doublet of apparent amylolytic activity (arrow G) is

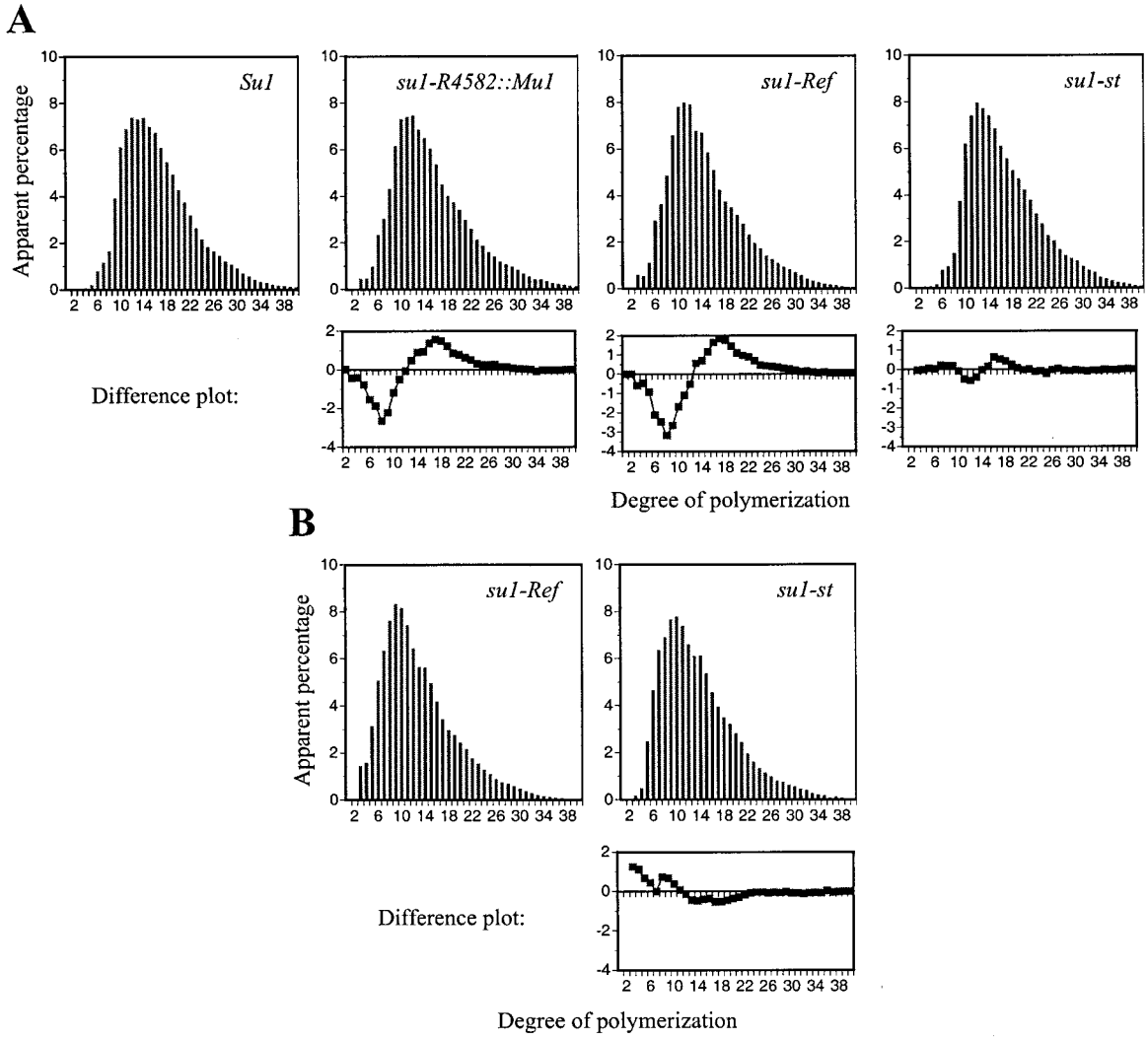

Figure 5. HPAEC-PAD analysis of chain length distributions. A, Amylopectin from *Su1*, *su1-R4582::Mu1*, *su1-Ref*, and *su1-st* homozygous kernels harvested 30 DAP was debranched with *Pseudomonas* isoamylase. Chain length distributions were determined using HPAEC-PAD and normalized to the total peak area. Differences in chain lengths of *su1-R4582::Mu1*, *su1-Ref*, and *su1-st* amylopectin-like molecules relative to *Su1* amylopectin are shown in difference plots below the respective mutant profiles. B, WSP from *su1-Ref* and *su1-st* kernels harvested 30 DAP was debranched and separated, as described for A. A difference plot comparing the WSP chain distributions is below the *su1-st* profile.

reduced in intensity in all three *su1-* mutant extracts, and the lower of these two bands is differentially affected by *su1-Ref*.

DISCUSSION

In this study, the direct molecular effects of three different *su1-* mutations on the isoamylase-type DBE specified by the gene were clearly determined. For *su1-R4582::Mu1*, the structure of the gene and lack of transcript indicate that the SU1 protein is completely missing in homozygous mutants. In contrast, both *su1-Ref* and *su1-st* produce transcripts that code for mutant SU1 polypeptides. Expression of *su1-Ref* appears to be normal at the level of mRNA accumulation, although the polypeptide abundance is reduced compared with wild type (Beatty et al., 1999). Thus, the $SU1^{Ref}$ mutant protein may be unstable relative to the wild-type SU1 protein. The fact that the kernel appearance and the chemical structure phenotype conditioned by *su1-Ref* closely resemble that caused by the null allele suggests that this mutant protein lacks enzymatic activity. SU1 isoamylase-type DBE activity was, in fact, shown to be severely reduced both in partially purified extracts (Beatty et al., 1999) and in the activity gels in this study. This loss of enzymatic activity is likely to result from the substitution in region IS-XII of the hydrophobic residue Trp, which is nearly universally conserved in all known isoamylase type enzymes by the charged residue Arg.

Despite their phenotypic similarities, differences do exist in the effects of *su1-Ref* and *su1-R4582::Mu1*. In

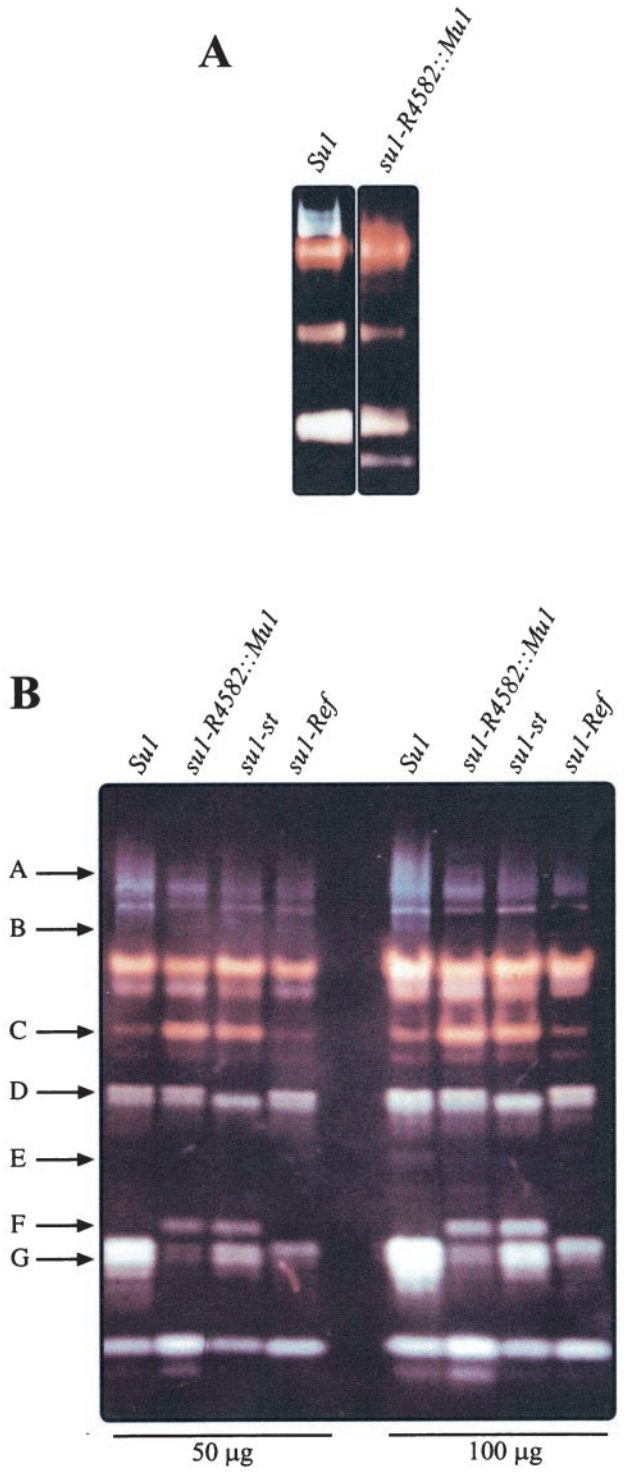

Figure 6. Native PAGE/activity gels (zymograms) of starch modifying activities. A, Twenty-five micrograms of total protein from *Su1* and *su1-R4582::Mu1* homozygous kernels harvested at 20 DAP was separated on a 5-cm native polyacrylamide gel, then electroblotted to a starch-containing gel. Starch modifying enzyme activities were visualized by staining with I_2/KI. B, Fifty or 100 μg total protein from *Su1*, *su1-R4582::Mu1*, *su1-st*, and *su1-Ref* homozygous kernels harvested at 20 DAP was analyzed as described for A on 15-cm native PAGE/activity gels. Arrows A through G indicate starch modifying activities that exhibit allele-specific variation.

particular, the former is dominant to *su1-st* with respect to kernel phenotype, whereas the latter is recessive. These differences may be explained by a complex effect of the *su1-st* allele on SU1 protein expression. The steady-state *su1-st* mRNA level is significantly reduced compared with wild type, and at least three different transcripts are produced from the mutant gene. Only two of these transcripts, type II and type III, are capable of producing full SU1 polypeptides, $SU1^{st\text{-}II}$, and $SU1^{st\text{-}III}$. At least one of these proteins must be present to explain the dominance of *su1-st* over the null allele *su1-R4582::Mu1*, although whether both forms accumulate cannot be discerned from these data. Furthermore, the mild kernel phenotype and intermediate chemical structure phenotype of homozygous *su1-st* kernels suggests that at least one of the $SU1^{st\text{-}II}$ and $SU1^{st\text{-}III}$ polypeptides possesses some enzymatic activity. This is likely to be a low level of activity, however, because the zymogram analysis showed the same result for *su1-st* and *su1-R4582::Mu1*. Alternatively, *su1-st* might not produce any active isoamylase-type DBE, in which case the partial function of this allele would have to be explained by a structural property of the polypeptide independent of starch hydrolytic activity.

The dominant/recessive relationships of the three mutant *su1* alleles are likely to be explained by the multimeric nature of the SU1 holoenzyme. The rice isoamylase-type DBE exists as a high M_r homomultimer, estimated to comprise four to six monomers (Fujita et al., 1999), and the maize enzyme also migrates as a high M_r complex in gel filtration chromatography (Beatty et al., 1999). Because *su1-R4582::Mu1* is a null allele, *su1-st/su1-R4582::Mu1* heterozygous kernels are expected to assemble a relatively small amount of SU1 isoamylase in a complex comprising $SU1^{st\text{-}II}$ and/or $SU1^{st\text{-}III}$, as would occur in homozygous *su1-st* kernels. Although such a complex would be reduced in abundance, it is likely to be enzymatically active and to provide some level of the DBE function needed for starch biosynthesis. The dominance of *su1-Ref* over *su1-st* most likely is explained by multimeric complexes containing $SU1^{Ref}$, $SU1^{st\text{-}II}$, and/or $SU1^{st\text{-}III}$, which we propose are inactive despite the presence of some potentially functional subunits. According to this hypothesis, the abundance of the $SU1^{st}$ subunits must be low relative to $SU1^{Ref}$, such that the occurrence of homomultimers lacking any $SU1^{Ref}$ subunits is very rare.

The potential production of two distinct mutant polypeptides from the *su1-st* gene is the consequence of the *Toad* element insertion within exon 10. The type-I transcript results from the skipping of exon 10 and the inserted *Toad* element during splicing. The splice donor and acceptor sites that border exon 10 are intact in the mutant, however, and the context of the sequence is such that they are not recognized by the splicing machinery. Plant introns normally are AU-rich, although the exons surrounding them are

GC-rich (Wiebauer et al., 1988). Intron recognition is thought to occur in part because of the high A+U composition of a sequence, but also because of discrete borders that separate AU-rich from GC-rich regions (Luehrsen et al., 1994; Lorkovic et al., 2000). The *Toad* TIRs are AU-rich (69%), so that their insertion into the small exon 10 sequence may mask the AU-rich/GC-rich borders that exist in the nonmutant *su1* gene. This would create a new, larger intron containing the exon 10 sequences. Additional examples of exon skipping and/or intron creation owing to AU-rich transposons are known. These include insertion of *Ds2* within the *Shrunken2* (*Sh2*) locus, creating *sh2-m1* (Giroux et al., 1994), insertion of *dSpm* within the *A2* locus, creating *a2-m1* (Menssen et al., 1990), and insertion of *dSpm* at the *Bronze1* locus, creating *bz1-m13* (Kim et al., 1987).

The AU-rich composition of the *Toad* TIRs also is likely to activate cryptic splice sites within the *Su1* sequence or the *Toad* element that result in formation of the type-II and type-III transcripts. Determination of 5′- and 3′-splice sites is mediated by downstream and upstream AU-rich tracts, respectively (Lou et al., 1993; McCullough et al., 1993). The *Su1* sequence normally contains both the D*1 cryptic donor site and the A* cryptic acceptor site (see Fig. 4), although neither is recognized by the splice machinery. Repositioning of the A* sequence downstream of the *Toad* insertion, as part of the host site duplication, changes the AU-environment of the sequence and enlarges the physical distance between it and either cryptic donor site (D*1 or D*2). Thus, these sites are used by the splicing machinery only when *Toad* is present.

The zymogram profiles of enzyme activities clearly show that the *su1* mutant alleles differ in their effects on specific BE activities and the activity of one or more amylolytic enzymes (Fig. 6). These observations suggest that the $SU1^{Ref}$ mutant polypeptide does have some functionality with respect to other enzymes, even if it lacks enzymatic function. One possible explanation is that either the SU1 or $SU1^{Ref}$ polypeptide can inhibit or alter the activities marked by arrows C and F in Figure 6, whether or not the proteins constitute an active isoamylase-type DBE. In contrast, *su1-R4582::Mu1* causes complete absence of the SU1 protein, which may explain the changes in these activities. Similarly, the *su1-st* mutation most likely results in accumulation of only a small amount of $SU1^{st\text{-}II}$ and/or $SU1^{st\text{-}III}$ polypeptide, and thus is likely to condition the same pleiotropic effects as the null allele. The unique effect of *su1-st* on the loss of a starch modifying activity indicated by arrow D in Figure 6, which is distinct from that of *Su1*, *su1-Ref*, or *su1-R4582::Mu1*, is likely to arise from a structural property of $SU1^{st\text{-}II}$ and/or $SU1^{st\text{-}III}$. This argument derives from the fact that this band does not vary depending on SU1 activity, because it is the same in the null mutant and the wild type. In summary, we propose that the overall function of the *su1* gene depends on (a) the level of enzymatic activity, (b) the level of the polypeptide independent of enzyme activity, and (c) specific structural properties of the SU1 polypeptide again unrelated to enzyme activity.

The *su1-Ref* and *su1-R4582::Mu1* mutations clearly affected the structure of amylopectin in starch granules with regard to the chain length distribution (Fig. 5). These data are consistent with the analysis of rice *su1-* mutants (Kubo et al., 1999), but differ from the analysis of Arabidopsis leaf starch in which an isoamylase mutation caused phytoglycogen accumulation without altering the structure of residual amylopectin (Zeeman et al., 1998). Both direct and indirect roles of DBE function in amylopectin biosynthesis have been proposed to account for the simultaneous occurrence of amylopectin and WSP in isoamylase-deficient mutants (Zeeman et al., 1998; Fujita et al., 1999; Myers et al., 2000). As far as can be determined from the activity gel profile, BEs are not altered significantly by *su1-Ref*, suggesting that changes in these enzymes are not responsible for the altered amylopectin structure. The change in chain length distribution is consistent with the hypothesis that the isoamylase-type DBE, and/or the pullulanase-type enzyme, directly modifies a precursor to amylopectin prior to its crystallization into the granule. One possibility is that the DBE(s) preferentially remove chains of a certain length, or chains positioned in some specific way within the newly branched region of the growing amylopectin molecule. An indirect role of the DBE, however, is not ruled out by these data. For example, the presence of phytoglycogen might alter the function of an SS or a BE, or altered supply of the substrates ADP-Glc or maltooligosaccharide might affect an SS activity such that it synthesizes chains of different lengths than normal.

The transcript characterization, the activity gel data, and the recessiveness of *su1-st* relative to *su1-Ref*, indicate that the level of isoamylase-type DBE activity is very low in *su1-st* mutants. The relatively mild kernel- and chemical structure phenotypes of *su1-st* homozygotes and *su1-st/su1-R4582::Mu1* heterozygotes, therefore, support the notion that only a very small amount of SU1 isoamylase is sufficient for synthesis of significant quantities of normal or near normal amylopectin. In nonmutant endosperm there may be an excess of isoamylase-type DBE activity over what is needed to produce wild-type levels of amylopectin. A major reduction in this enzyme in *su1-st* mutants may still leave enough function to produce significant quantities of starch, as was seen in the 30 DAP kernels from the 1997-growing season. The variability in *su1-st* expressivity may be explained by environmental factors affecting the threshold level of isoamylase-type DBE activity required for normal starch biosynthesis.

This study has provided new information about the effects of mutations in the isoamylase-type DBE.

The observation of numerous allele-specific effects on starch structure and the activities of other starch modifying enzymes implicates both enzymatic and nonenzymatic features of the SU1 polypeptide in starch biosynthesis. We expect that the pleiotropic effects of the *su1-* mutations are indicative of fundamental aspects of the starch biosynthetic mechanism.

MATERIALS AND METHODS

Plant Materials and Nomenclature

The nomenclature follows the standard maize (*Zea mays*) genetics format (Beavis et al., 1995). The mutant allele *su1-st* arose spontaneously in a population of Krug's yellow dent corn (Dahlstrom and Lonnquist, 1964) and was generously provided by Dr. Oliver Nelson (University of Wisconsin, Madison). All *su1-* mutant alleles were introgressed into the W64A inbred background by five generations of back crossing to the standard line.

RNA Gel-Blot Analyses

Total RNA was isolated from maize kernels harvested 20 DAP and subjected to gel-blot analysis as described previously (James et al., 1995; Gao et al., 1996). RNA gel blots were hybridized with a 387-bp antisense RNA probe from the 3′ end of the Su1 cDNA. The probe was synthesized as an in vitro run-off transcription product using the StripEZ T7 kit (catalog no. 1362, Ambion, Austin, TX). The transcription template was plasmid pSu1(BS), linearized at the unique *Bgl*II site within the Su1 cDNA. The RNA probe corresponds to nt 2,608 to nt 2,221 of the Su1 cDNA sequence (GenBank accession no. U18908) running in the antisense direction.

PCR, RT-PCR, and DNA Sequence Analysis

Sequencing of the *su1-Ref* coding sequence followed PCR and RT-PCR amplifications. PCR amplification of *su1-Ref* genomic DNA was used to obtain 5′-end sequence information with the primer pair JD01 (5′-GGC TCC CTC CCC TCC ACT TCC-3′) and 452 (5′- GGG ATC ATA CCA GCC ATT TGA-3′). Downstream sequence information for *su1-Ref* and *su1-st* was obtained following RT-PCR amplification of mRNA using the following primer pairs: 797 (5′-CTC AAA TGG CTG GTA TGA-3′) and JD02 (5′-CCA TTC CAC TCT GAC CAA ACG-3′); MB02A (5′-GGG GAA AAT CAT AAT CTT A-3′) and MB02 N (5′-TGG TAG ACG GTG ACA GCA-3′); JD03 (5′-ATT GTT CTT CCT TCT TAT CCC-3′) and MB03D (5′-TTG GTC AGA GTG GAA TGG-3′); JD18 (5′-ACC AGA GGA TGC AGT CTA TG-3′) and JD03. Primers JD19 (5′-TCC TTA TTT TGT CTT TTT AGG CAT TCT-3′) and JD20 (5′-GCA GAT GTT GGG AGG GTT AGT GTC T-3′) were used for PCR amplification of *su1-st* genomic DNA containing the *Toad* sequence. Template mRNA for RT-PCR was purified from total RNA using the PolyA+ Tract mRNA isolation system (catalog no. Z5300, Promega, Madison, WI). The HF One-step RT-PCR System (catalog no. 600164, Stratagene, La Jolla, CA) was used for the RT-PCR. Sequences were determined directly from the PCR products, except for the type-II and type-III transcripts produced from *su1-st* by the JD18/JD03 primer pair. In those instances the PCR products were first cloned using the pGEM-Teasy vector system (catalog no. A1360, Promega) and then sequenced from the recombinant plasmids. The amplification product from the JD19/JD20 primer pair, containing the *Toad* element and flanking su1 genomic sequences, also was cloned in the vector system, producing plasmid pJD19. Computational analyses were performed using the GCG Sequence Analysis Software Package (Genetics Computer Group, Madison, WI).

DNA Gel-Blot Analysis

Genomic DNAs were isolated from seedling leaves of a homozygous *su1-st* plant in the W64A background and inbred lines W64A, Oh43, Mo17, B73, and F_1 hybrids B77/B79 and Q66/Q67 according to published procedure (Dellaporta et al., 1983), digested with *Bam*HI and *Eco*RI, electrophoresed, and transferred to nylon membranes. The blots were hybridized at 65°C in a buffer of 5× SSC, 5× Denhardt's solution, 0.1% (w/v) SDS, and 10 μg mL^{-1} sonicated, denatured salmon sperm DNA. The hybridization probe was the 0.5-kb *Eco*RI/*Pvu*II fragment from pJD19 (containing the central portion of the *Toad* element and one TIR), labeled with ^{32}P using the RTS Radprime Kit (catalog no. 10387–017, Life Technologies/Gibco-BRL, Cleveland). Blots were washed one time in 2× SSC, 0.1% (w/v) SDS at 65°C for 15 min and once in 0.2× SSC, 0.1% (w/v) SDS at 65°C for 15 min.

Carbohydrate Extraction and Quantification

Immature kernels were harvested 20 to 30 DAP and stored at −80°C. Insoluble starch and soluble carbohydrates were extracted from five whole kernels as follows. After removal of the pericarp and embryo by dissection, endosperm tissue was ground in water in a chilled mortar and pestle, and the volume was brought to 4 mL. Water was removed from a 1-mL portion of the homogenate by drying in an oven at 70°C, and the kernel dry weight was determined from the remaining material. The remaining 3-mL portion of the homogenate was centrifuged at 10,000*g* for 5 min. The pellet was washed in cold water and again centrifuged at 10,000*g* for 5 min. The supernatant fractions from both centrifugations, containing soluble carbohydrates, were pooled and incubated in a boiling water bath for 10 min. The pellet fraction, consisting mostly of insoluble starch granules, was dissolved in 100% (v/v) dimethyl sulfoxide (DMSO) and incubated in a boiling water bath for 30 min.

Total glucan oligomer or polymer content was measured in terms of milligram carbohydrate/gram dry weight following complete digestion of the insoluble starch fraction and the soluble carbohydrate fraction with amyloglucosidase. These assays used a commercial Glc assay kit (catalog no. 207748, Boehringer Mannheim, Basel) according to the manufacturer's protocol. The quantities of Suc, D-Fru, and

D-Glc were measured in terms of milligram carbohydrate/gram dry weight by specific enzymatic assays (catalog no. 716260, Boehringer Mannheim).

Starch Structural Analysis

Approximately 20 mg Glc equivalents of solubilized granular starch in 100% (v/v) DMSO was precipitated by overnight incubation in 4 volumes absolute ethanol at −20°C. During this step, we presume that lipids have been removed from the carbohydrate fraction. After centrifugation at 2,000*g* for 5 min, the pellet was dissolved in 2 mL of 10 mM NaOH. Amylopectin and amylose were separated by gel permeation chromatography on Sepharose CL-2B columns (1.8-m height; 1.8-cm diameter). Samples were eluted with 10 mM NaOH at a rate of 30 mL/h. Aliquots of each 3-mL fraction (100 μL) were mixed with 400 μL of I_2/KI (0.67% [w/v] I_2 and 3.33% [w/v] KI) solution, and maximal absorbance was determined by measuring the spectrum from 400 to 700 nm. Fractions containing amylopectin or amylose were pooled, dialyzed against water at 4°C, lyophilized, and stored at room temperature.

Characterization of the chain length distribution by HPAEC-PAD chromatography was performed as previously described (Fontaine et al., 1993). Briefly, the lyophilized amylopectin obtained from the gel permeation column was dissolved in 90% (v/v) DMSO, quantified, diluted to 1 mg mL^{-1}, and digested to completion with 0.2 units mL^{-1} *Pseudomonas* sp isoamylase (catalog no. E-ISAMY, Megazyme International, Bray, County Wicklow, Ireland) during an overnight incubation at 45°C. Samples (50 μL) were injected into the Dionex HPAEC-PAD system for characterization of the chain length distribution. The area under each peak of chain length 3 to 40 Glc units was integrated and the apparent frequency of each chain length was calculated as the percentage of total peak area.

Activity Gel Analysis of Starch Modifying Enzymes

Frozen kernels (5 g) were ground to a fine powder in liquid nitrogen with a mortar and pestle, and the tissue was suspended in 5 mL of buffer containing 50 mM sodium acetate, pH 6, 20 mM dithiothreitol. All of the lysates were centrifuged at 50,000*g* for 1 h at 4°C, which removes phytoglycogen from the *su1-* mutant extracts. The supernatant was stored at −80°C. Total proteins (50 or 100 μg) were separated on a native polyacrylamide gel (16 cm × 20 cm × 0.15 cm). The resolving gel contained 7% (w/v) acrylamide (29:1 acrylamide-bisacrylamide was used throughout) and 375 mM Tris-HCl, pH 8.8. The stacking gel contained 4% (w/v) acrylamide and 63 mM Tris-HCl, pH 6.8. Electrophoresis was conducted at 4°C, 25 V cm^{-1} for 4 h using a Protean II cell (Bio-Rad Laboratories, Hercules, CA) in an electrode buffer of 25 mM Tris, 192 mM Gly, pH 8.8, and 2 mM dithiothreitol. At the end of the run, the gel was electroblotted to a polacrylamide gel of the same size containing 7% (w/v) acrylamide, 0.3% (w/v) potato starch (Sigma, St. Louis), and 375 mM Tris-HCl, pH 8.8. The transfer was performed overnight at 20 V in the electrode buffer at room temperature. Starch metabolic activities were observed by staining the gel with I_2/KI solution, and the gel was photographed immediately. The 5-cm activity gels were identical except that the Mini-Protean II cell (Bio-Rad Laboratories) was used, 25 μg of the sample was applied, and electrophoresis was for 45 min.

ACKNOWLEDGMENTS

We thank Oliver Nelson for providing the original *su1-st* material, Katie Dilks for technical assistance in carbohydrate analysis, and Paul Scott for assistance with HPAEC-PAD analysis. Nucleotide sequencing was performed at the Iowa State University Nucleic Acid Sequencing and Synthesis Facility.

Received November 3, 2000; returned for revision December 15, 2000; accepted December 21, 2000.

LITERATURE CITED

Beatty MK, Myers AM, James MG (1997) Genomic nucleotide sequence of a full-length wild type allele of the maize *sugary1 (su1)* gene (accession no. AF030882) (PGR 97–187). Plant Physiol **115:** 1731

Beatty MK, Rahman A, Cao H, Woodman W, Lee M, Myers AM, James MG (1999) Purification and molecular genetic characterization of ZPU1, a pullulanase-type starch debranching enzyme from maize. Plant Physiol **119:** 255–266

Beavis W, Berlyn M, Burr B, Chandler V, Coe E, Fauron C, Nelson O, Polacco M, Rodermel S, Sachs M et al. (1995) A standard for maize genetics nomenclature. Maize Genet Coop Newsl **69:** 182–184

Correns C (1901) Bastarde zwischen maisrassen, mit besonder Berucksichtung der Xenien. Bibliotheca Bot **53:** 1–161

Creech RG (1968) Carbohydrate synthesis in maize. Adv Agron **20:** 275–322

Dahlstrom DE, Lonnquist JH (1964) A new allele at the sugary-1 locus in maize. J Hered **55:** 242–246

Dauvillee D, Mestre V, Colleoni C, Slomianny M-C, Mouille G, Delrue B, d'Hulst C, Bliard C, Nuzillard J-M, Ball S (2000) The debranching enzyme complex missing in glycogen accumulating mutants of *Chlamydomonas reinhardtii* displays an isoamylase-type specificity. Plant Sci **157:** 145–156

Dellaporta SL, Wood J, Hicks JB (1983) A plant version of DNA minipreparation: version II. Plant Mol Biol Rep **1:** 19–21

Doehlert DC, Knutson CA (1991) Two classes of starch debranching enzymes from developing maize kernels. J Plant Physiol **138:** 566–572

Federoff N (1989) Maize transposable elements. *In* D Berg, M Howe, eds, Mobile DNA. American Society of Microbiology, Washington, DC, pp 375–411

Finnegan DJ (1989) Eukaryotic transposable elements and genome evolution. Trends Genet **5:** 103–107

Fontaine T, Hulst CD, Maddelein M-L, Routier F, Pepin TM, Decq A, Wieruszeski J-M, Delrue B, Van den

Koornhuyse N, Bossu J-P et al. (1993) Toward an understanding of the biogenesis of the starch granule. J Biol Chem **268:** 16223–16230

Fujita N, Kubo A, Francisco PB, Nakakita M, Harada K, Minaka N, Nakamura Y (1999) Purification, characterization, and cDNA structure of isoamylase from developing endosperm of rice. Planta **208:** 283–293

Gallant DJ, Bouchet B, Baldwin PM (1997) Microscopy of starch: evidence of a new level of granule organization. Carbohydr Polym **32:** 177–191

Gao M, Fisher DK, Kim K-N, Shannon JC, Guiltinan MJ (1996) Evolutionary conservation and expression patterns of maize starch branching enzyme I and IIb genes suggests isoform specialization. Plant Mol Biol **30:** 1223–1232

Giroux MJ, Clancy M, Baier J, Ingham L, McCarty D, Hannah LC (1994) De novo synthesis of an intron by the maize transposable element dissociation. Proc Natl Acad Sci USA **91:** 12150–12154

Hodges HF, Creech RG, Loerch JD (1969) Biosynthesis of phytoglycogen in maize endosperm: the branching enzyme. Biochim Biophys Acta **185:** 70–79

Imberty A, Buleon A, Tran V, Perez S (1991) Recent advances in knowledge of starch structure. Starch/Staerke **43:** 375–384

James MG, Robertson DS, Myers AM (1995) Characterization of the maize gene *sugary1*, a determinant of starch composition in kernels. Plant Cell **7:** 417–429

Jesperson HM, MacGregor EA, Henrissat B, Sierks MR, Svensson B (1993) Starch- and glycogen-debranching and branching enzymes: prediction of structural features of the catalytic (β/α)8-barrel domain and evolutionary relationship to other amylolytic enzymes. J Protein Chem **12:** 791–805

Kim HY, Schiefelbein JW, Raboy V, Furtek DB, Nelson OE Jr (1987) RNA splicing permits expression of a maize gene with a defective suppressor-mutator transposable element insertion in an exon. Proc Natl Acad Sci USA **84:** 5863–5867

Kossman J, Lloyd J (2000) Understanding and influencing starch biochemistry. Crit Rev Biochem Mol Biol **35:** 141–196

Kubo A, Fujita N, Harada K, Matsuda T, Satoh H, Nakamura Y (1999) The starch-debranching enzymes isoamylase and pullulanase are both involved in amylopectin biosynthesis in rice endosperm. Plant Physiol **121:** 399–409

Lavintman N (1966) The formation of branched glucans in sweet corn. Arch Biochem Biophys **116:** 1–8

Lee EYC, Whelan WJ (1971) Glycogen and starch debranching enyzmes. *In* P Boyer, ed, The Enzymes, Vol 5. Academic Press, New York, pp 191–234

Lorkovic ZJ, Kirk DAW, Lambermon MHL, Filipowicz W (2000) Pre-mRNA splicing in higher plants. Trends Plant Sci **5:** 160–167

Lou H, McCullough AJ, Schuler MA (1993) 3′-Splice site selection in dicot plant nuclei is position dependent. Mol Cell Biol **13:** 4485–4493

Luehrsen KR, Taha S, Walbot V (1994) Nuclear pre-RNA processing in higher plants. Prog Nucleic Acids Res Mol Biol **47:** 149–193

Manners D (1997) Observations on the specificity and nomenclature of starch debranching enzymes. J Appl Glycosci **44:** 83–85

McCullough AJ, Lou H, Schuler MA (1993) Factors affecting authentic 5′-splice site selection in plant nuclei. Mol Cell Biol **13:** 1323–1331

Menssen A, Hohmann S, Martin W, Schnable PS, Peterson PA, Saedler H, Gierl A (1990) The En/Spm transposable element of *Zea mays* contains splice sites at the termini generating a novel intron from a dSpm element in the A2 gene. EMBO J **9:** 3051–7

Morris DZ, Morris CT (1939) Glycogen in the seed of *Zea mays*. J Biol Chem **130:** 535–544

Mouille G, Maddelein M-L, Libessart N, Talaga P, Decq A, Delrue B, Ball S (1996) Preamylopectin processing: a mandatory step for starch biosynthesis in plants. Plant Cell **8:** 1353–1366

Myers AM, Morell MK, James MG, Ball SG (2000) Recent progress toward understanding the amylopectin crystal. Plant Physiol **122:** 989–997

Nakamura Y, Umemoto T, Takahata Y, Komae K, Amano E, Satoh H (1996) Changes in structure of starch and enzyme activities affected by sugary mutations in developing rice endosperm: possible role of starch debranching enzyme (R-enzyme) in amylopectin biosynthesis. Physiol Plant **97:** 491–498

Nevers P, Shepherd NS, Saedler H (1986) Plant transposable elements. Adv Bot Res **12:** 103–203

Pan D, Nelson OE (1984) A debranching enzyme deficiency in endosperms of the *sugary-1* mutants of maize. Plant Physiol **74:** 324–328

Rahman A, Wong K-S, Jane J-L, Myers AM, James MG (1998) Characterization of SU1 isoamylase, a determinant of storage starch structure in maize. Plant Physiol **117:** 425–435

Shannon JC, Garwood DL (1984) Genetics and physiology of starch development. *In* RL Whistler, JN Bemiller, EF Paschall, eds, Starch: Chemistry and Technology. Academic Press, Orlando, FL, pp 25–86

Smith AM (1999) Making starch. Curr Opin Plant Biol **2:** 223–229

Tomalsky DS, Krisman CR (1987) The degree of branching in (α1, 4)-(α1, 6)-linked glucopolysaccharides is dependent on intrinsic properties of the branching enzymes. Eur J Biochem **168:** 393–397

Wiebauer K, Herrero JJ, Filipowicz W (1988) Nuclear premRNA processing in plants: distinct modes of 3′-splicesite selection in plants and animals. Mol Cell Biol **8:** 2042–51

Yun S, Matheson NK (1993) Structures of the amylopectins of waxy, normal, amylose-extender, and wx:ae genotypes and of the phytoglycogen of maize. Carbohydr Res **243:** 307–321

Zeeman SC, Umemoto T, Lue W-L, Au-Yeung P, Martin C, Smith AM, Chen J (1998) A mutant of *Arabidopsis* lacking a chloroplastic isoamylase accumulates both starch and phytoglycogen. Plant Cell **10:** 1699–1711